
On the Neural Tangent Kernel of Deep Networks with Orthogonal Initialization

Wei Huang*

University of Technology Sydney, Australia
wei.huang-6@student.uts.edu.au

Weitao Du*

Northwestern University, USA
weitao.du@northwestern.edu

Richard Yi Da Xu

University of Technology Sydney, Australia
YiDa.Xu@uts.edu.au

Abstract

In recent years, a critical initialization scheme with orthogonal initialization deep nonlinear networks has been proposed. The orthogonal weights are crucial to achieve *dynamical isometry* for random networks, where entire spectrum of singular values of an input-output Jacobian are around one. The strong empirical evidence that orthogonal initialization in linear networks and the linear regime of non-linear networks can speed up training than Gaussian networks raise great interests. One recent work has proven the benefit of orthogonal initialization in linear networks. However, the dynamics behind it have not been revealed on non-linear networks. In this work, we study the Neural Tangent Kernel (NTK), which describes the gradient descent training of wide networks, on orthogonal, wide, fully-connect, and nonlinear networks. We prove that NTK of Gaussian and Orthogonal weights are equal when the network width is infinite, resulting in a conclusion that orthogonal initialization can speed up training is a finite-width effect in the small learning rate region. Then we find that during training, the NTK of infinite-width networks with orthogonal initialization stay constant theoretically and vary at a rate of the same order empirically as Gaussian ones, as the width tends to infinity. Finally, we conduct a thorough empirical investigation of training speed on CIFAR10 datasets and show the benefit of orthogonal initialization lies in the large learning rate and depth region in a linear regime of nonlinear networks.

1 Introduction

Deep learning has gained state-of-the-art performance in many fields, including computer vision [1], natural language processing [2], and reinforcement learning [3]. An array of innovative techniques of neural networks such as residual connections [4], dropout [5], and batch normalization [6] contributed to the prosperity of deep learning. Recently, the mean field theory [7, 8] opens a gate to analyze the principle behind neural networks by looking at random, infinite width, and fully-connected networks. This analysis has been extended to a wide range of architectures, i.e. convolutional networks [9], recurrent networks [10], dropout networks [11], residual networks [12], batch normalization [13].

A critical initialization that can have infinity length-scale in signal propagation and avoid gradient vanishing and exploding problem during gradient back-propagation at initialization has been found through mean field theory and verified empirically [8]. This critical initialization requires the mean squared singular value of a network’s input-output Jacobian is $O(1)$. On the basis of this line of work,

*Both authors contributed equally to this work.

[14, 15] proposed that ensuring all singular values of the Jacobian are concentrated near one can yield a speed-up in learning with tools of free probability and random matrix theory. The improved initialization is known as *dynamical isometry*, derived from the study of dynamics of linear networks [16]. Later, dynamical isometry was introduced to a range of architectures such as residual networks [17, 18], convolutional networks [9], recurrent networks [10] and show that an excellent performance on real datasets.

The benefit of the orthogonality in linear networks has been proven recently [19]. However, the dynamics of nonlinear networks with orthogonal initialization has rarely been investigated. In the nonlinear setting, it is impossible to derive an analytic expression for the dynamics of the loss function. To fill this gap, we refer to a recent technique called Neural Tangent Kernel (NTK) [20] as a promising tool. NTK is a kernel characterized by a derivative of the output of networks to its parameters. Researchers show that it converges to a deterministic kernel and keeps unchanged during gradient descent in the infinite-width networks [20], thus can describe the dynamics of infinite-width networks through a set of ordinary differential equations. It is equivalent to say that, in the infinite width limit, networks are governed by a linear model and excellent empirical agreement between the predictions of the original network and those of the linearized version for finite practically-sized networks [21].

We first prove that the NTK of networks with orthogonal initialization converges to an identical and deterministic kernel as Gaussian's. This conclusion reveals there is no benefit of orthogonality in the small learning rate regime for infinity-width networks. Then we find that during training, the NTK of infinite-width network with orthogonal initialization stays constant theoretically and varies at a rate of the same order in large finite-width as Gaussian ones empirically. This implies that there is no significant difference between orthogonal and Gaussian initialization of wide networks with a small learning rate during training. Finally, we conduct a thorough empirical investigation of training speed on CIFAR10 datasets and show the orthogonal initialization may hinder training speed in the large learning rate and depth phase in a linear regime of nonlinear networks.

2 Related Work

A recent work [19] investigated orthogonal initialization on the linear network. They provided a rigorous proof that drawing the initial weights from the orthogonal group speeds up convergence relative to the standard Gaussian initialization. However, our work is to address the nonlinear activation, which is more complicated due to the nonlinear nature of deep neural networks. Another work [22] has tempted to explain why dynamical isometry equipped with orthogonal initialization has achieved significant success. They showed a connection between the maximum curvature of the optimization landscape as measured by the Fisher information matrix (FIM) and the spectral radius of the input-output Jacobian, which partially explains why more isometric networks can train much faster. Even that NTK and FIM have the same spectrum, our works provide a more precise characterization of the dynamics of wide networks.

The original work of Neural Tangent Kernel [20] has shown that in the infinite-width limit, NTK converges to an explicit limiting kernel, and it stays constant during training for Gaussian initialization. We extend this result to the orthogonal initialization and show that they are the same kernel in the infinite width limit. Further, the following work [21] has achieved the same conclusion through a different statement that gradient descent dynamics of the original neural network falls into its linearized dynamics regime. We adopt the similar proof strategy from [21] to state that NTK will stay constant in networks with orthogonal initialization during training. While the original work of NTK is groundbreaking in producing an equation to predict the behavior of gradient descent in the small learning rate, wide width regime, its proof is incomplete as it implicitly assumes gradient independence. To fill this gap [23] provides a complete proof. Besides, both works [24, 25] have proven the same proprieties of NTK in the infinite-width limit in different ways. However, all the works focus on the Gaussian initialization.

Common works of NTK adopt a so called ntk parameterization [20], since the standard parameterization can lead to divergent gradient flow in the infinite limit. To account for this problem, an improved standard parameterization has been proposed [26]. In this work, we focus on both the standard parameterization and ntk parameterization for orthogonal initialization. A python library name Neural Tangents enables research into infinite-width and finite-width with numerical method

neural networks [27]. Both improved standard and ntk parameterization are equipped in Neural Tangents. We add some codes to realize orthogonal initialization on the basis of Neural Tangents to perform experiments in our work.

3 Preliminaries

3.1 Networks

Consider a fully-connected network of L layers of widths n_l , for $l = 0, \dots, L$, where $l = 0$ is the input layer and $l = L$ is output layer. Following the typical nomenclature of literature, we denote synaptic weight and bias for the l -th layer by $W^l \in \mathbb{R}^{n_l \times n_{l-1}}$ and $b^l \in \mathbb{R}^{n_l}$, with a point-wise activations function $\phi : \mathbb{R} \rightarrow \mathbb{R}$. Suppose there are D training points denoted by $\{(x_d, y_d)\}_{d=1}^D$, where input $X = (x_1, \dots, x_D) \in \mathbb{R}^{n_0 \times D}$, and label $Y = (y_1, \dots, y_D) \in \mathbb{R}^{n_L \times D}$.

For each input $x \in \mathbb{R}^{n_0}$, pre-activations and post-activations are denoted by $h^l(x) \in \mathbb{R}^{n_l}$ and $x^l(x) \in \mathbb{R}^{n_l}$ respectively. The information propagation in this network is govern by,

$$x^l = \phi(h^l), \quad h^l = W^l x^{l-1} + b^l, \quad (1)$$

3.2 Gaussian initialization

Standard parameterization requires the parameter set $\theta = \{W_{ij}^l, b_i^l\}$ is an ensemble generated by,

$$W_{ij}^l \sim \mathcal{N}(0, \frac{\sigma_w^2}{n_{l-1}}), \quad b_i^l \sim \mathcal{N}(0, \sigma_b^2), \quad (2)$$

where σ_w^2 and σ_b^2 are weight and bias variances. The variance of weights is scaled by the width of previous layer n_{l-1} is to preserve the order of post-activations layer to be $O(1)$. Suppose the L_2 norm of previous layer, σ_w^2 , and σ_b^2 is of $O(1)$, i. e. $\|x^{l-1}\|_2^2, \sigma_w^2, \sigma_b^2 \sim O(1)$, then we have,

$$\begin{aligned} \mathbb{E}[\|h^l\|_2^2] &= \mathbb{E}\left[\frac{1}{n_l} \sum_{i=1}^{n_l} (h_i^l)^2\right] = \mathbb{E}\left[\frac{1}{n_l} [(W^l x^{l-1})^T W^l x^{l-1} + (b^l)^T b^l]\right] \\ &= \mathbb{E}\left[\frac{1}{n_l} [(x^{l-1})^T \sum_{j=1}^{n_l} (W_{ij}^l)^T W_{jk}^l x^{l-1} + (b^l)^T b^l]\right] = \frac{\sigma_w^2}{n_{l-1}} \sum_{i=1}^{n_{l-1}} (x_i^{l-1})^2 + \sigma_b^2 \sim O(1) \end{aligned} \quad (3)$$

We denote the parameterization of Equation (2) as *standard parameterization*. However, this parameterization can lead to a divergence in derivation of neural tangent kernel. To overcome this problem, *ntk parameterization* was introduced,

$$W_{ij}^l = \frac{\sigma_w}{\sqrt{n_{l-1}}} \omega_{ij}^l, \quad b_i^l = \sigma_b \beta_i^l, \quad (4)$$

where $\omega_{ij}^l, \beta_i^l \sim \mathcal{N}(0, 1)$. Unlike the standard parameterization that only normalizes the forward dynamics of the network, the ntk parameterization also normalizes its backward dynamics to prevent divergence[20, 21]. Note that the training and testing dynamics of these two parameterization can be identical if the learning rate is set with a width-dependent scaling factor, more details regarding learning setting can be found in [21].

3.3 Orthogonal initialization

The premise of realizing dynamical isometry in fully connected networks is to adopt random orthogonal initialization for weights [14]. It is drawn from a uniform distribution over scaled orthogonal matrices obeying,

$$(W^l)^T W^l = \sigma_w^2 \mathbf{I}, \quad (5)$$

Note that this is the *standard parameterization* for orthogonal weights, and the orthogonal version of *ntk parameterization* can be written as,

$$W_{ij}^l = \frac{\sigma_w}{\sqrt{n_{l-1}}} \omega_{ij}^l, \quad (\omega_{ij}^l)^T \omega_{ij}^l = n_{l-1} \mathbf{I}. \quad (6)$$

Similar to the Gaussian weights, we provide a simple argument for that orthogonal initialization can have the L_2 norms of the output of each layer are of order one as well,

$$\begin{aligned}\mathbb{E}[\|h^l\|_2^2] &= \mathbb{E}\left[\frac{1}{n_l} \sum_{i=1}^{n_l} (h_i^l)^2\right] = \mathbb{E}\left[\frac{1}{n_l} [(W^l x^{l-1})^T W^l x^{l-1} + (b^l)^T b^l]\right] \\ &= \mathbb{E}\left[\frac{1}{n_l} [(x^{l-1})^T \sum_{j=1}^{n_l} (W_{ij}^l)^T W_{jk}^l x^{l-1} + (b^l)^T b^l]\right] = \frac{\sigma_w^2}{n_l} \sum_{i=1}^{n_{l-1}} (x_i^{l-1})^2 + \sigma_b^2 \sim O(1)\end{aligned}\tag{7}$$

Note that the denominator is a little different from that of Gaussian. When the width of connected layers, i.e. n_{l-1} and n_l are different, we need an extra scale factor $\frac{n_l}{n_{l-1}}$ to make the two initialization have the exact same order of norm. Finally, we show a summary of both (improved) standard parameterization and ntk parameterization of Gaussian and orthogonal initialization in Table 1. The factor s in layer equation of standard parameterization is introduced to prevent divergence of NTK [26]. The core idea is to write the width of the neural network in each layer in terms of an auxiliary parameter, s , $n^l = sN^l$. Instead of letting $n^l \rightarrow \infty$, we adopt s as the limiting factor. The same strategy can be applied to the orthogonal ntk parameterization, and term N_{l-1} is hidden in the identity matrix, i.e. $\mathbf{I}_{N_{l-1} \times N_{l-1}}$.

Table 1: Summary of both (improved) standard parameterization and ntk parameterization of Gaussian and orthogonal initialization. The abbreviation ‘‘std’’ stands for standard, and the parameterization is omitted after ntk or std.

Parameterization	Gaussian ntk	Gaussian std	Orthogonal ntk	Orthogonal std
W initialization	$\omega \sim \mathcal{N}(0, 1)$	$W \sim \mathcal{N}(0, \frac{\sigma_w^2}{N_{l-1}})$	$(\omega^l)^T \omega^l = n_{l-1} \mathbf{I}$	$W^T W = \sigma_w^2 \mathbf{I}$
b initialization	$\beta \sim \mathcal{N}(0, 1)$	$b \sim \mathcal{N}(0, \sigma_b^2)$	$\beta \sim \mathcal{N}(0, 1)$	$b \sim \mathcal{N}(0, \sigma_b^2)$
layer equation	$\frac{\sigma_w}{\sqrt{n_{l-1}}} \omega^l x^{l-1} + \sigma_b \beta^l$	$\frac{1}{\sqrt{s}} W^l x^{l-1} + b^l$	$\frac{\sigma_w}{\sqrt{n_{l-1}}} \omega^l x^{l-1} + \sigma_b \beta^l$	$\frac{1}{\sqrt{s}} W^l x^{l-1} + b^l$

3.4 Neural Tangent Kernel

The neural tangent kernel (NTK) was originated from [20] and defined as,

$$\Theta_t(X, X) = \nabla_{\theta} f_t(\theta, X) \nabla_{\theta} f_t(\theta, X)^T.\tag{8}$$

where the function f_t is the outputs of the network at training time t , i.e. $f_t(\theta, X) = h_t^L(\theta, X) \in \mathbb{R}^{D_{n_L}}$, and $\nabla_{\theta} f_t(\theta, X) = \text{vec}([\nabla_{\theta} f_t(\theta, x)]_{x \in X}) \in \mathbb{R}^{D_{n_L}}$. Thus, the neural tangent kernel is formulated as a $D_{n_L} \times D_{n_L}$ matrix.

The original NTK work [20] studied the behavior of the output of the neural network f_t regarding to NTK in the infinite-width limit when the network is trained using a gradient descent algorithm. Later, [21] present this result in another statement that infinite width networks are linearized networks in the parameter space. We recall some of these results here.

Let η be the learning rate, and \mathcal{L} be the loss function. Then dynamic of gradient flow for parameters and output function is given by,

$$\begin{aligned}\frac{\partial \theta}{\partial t} &= -\eta \nabla_{\theta} \mathcal{L} = -\eta \nabla_{\theta} f_t(\theta, X)^T \nabla_{f_t(\theta, X)} \mathcal{L} \\ \frac{\partial f_t(\theta, x)}{\partial t} &= \nabla_{\theta} f_t(\theta, x) \frac{\partial \theta}{\partial t} = -\eta \Theta_t(x, X) \nabla_{f_t(\theta, X)} \mathcal{L}.\end{aligned}\tag{9}$$

This equation for f_t has no substantial insight in studying the behavior of networks, since $\Theta_t(x, X)$ varies with time evolution of training. However, as stated in above, the ntk $\Theta_t(X, X)$ converges to a deterministic kernel $\Theta_{\infty}(X, X)$ and does not change during training, in the infinite-width limit, i.e. $\Theta_t(X, X) = \Theta_{\infty}(X, X)$. As a result, the infinite width limit of the training dynamics is given by ,

$$\frac{\partial f_t(\theta, x)}{\partial t} = -\eta \Theta_{\infty}(x, X) \nabla_{f_t(\theta, X)} \mathcal{L}.\tag{10}$$

In the case of an MSE loss, $\mathcal{L}(y, f) = \frac{1}{2} \|y - f_t(\theta, x)\|_2^2$, then the Equation (10) becomes a linear model with a solution,

$$f_t(\theta, X) = (\mathbf{I} - e^{-\eta\Theta_\infty(X, X)})Y + e^{-\eta\Theta_\infty(X, X)}f_0(\theta, X). \quad (11)$$

This equivalent to replace the outputs of the neural network by their first order Taylor expansion in the parameter space,

$$f_t(\theta_t, x) = f_0(\theta_0, x) + \nabla_{\theta_0} f_0(\theta_0, x)(\theta_t - \theta_0). \quad (12)$$

4 Theoretical results

4.1 Networks with orthogonal initialization is a Gaussian process in the infinite width limit

As stated in [28, 29], the pre-activation h_i^l of Gaussian initialized network for each hidden layer, i.e. $l = 1, \dots, L - 1$ tend to i.i.d Gaussian processes in the infinite-width limit. Note that this is the proposition to construct the neural tangent kernel in Networks with Gaussian weights [20]. We extend this proposition to the orthogonal initialization case:

Proposition 1. *For a network of depth L at initialization, with a Lipschitz nonlinearity ϕ , and in the limit as $n_1, \dots, n_{L-1} \rightarrow \infty$, the pre-activation h_i^l , for $i = 1, \dots, n_l$, tend to i.i.d centered Gaussian processes of covariance Σ^l , where Σ^l is defined recursively by:*

$$\begin{aligned} \Sigma^1(x, x') &= \frac{\sigma_w^2}{n_0} x^T x' + \sigma_b^2 \\ \Sigma^l(x, x') &= \sigma_w^2 \mathbb{E}_{f \sim \mathcal{N}(0, \Sigma^{l-1})} [\phi(f(x))\phi(f(x'))] + \sigma_b^2, \end{aligned}$$

taking the expectation with respect to a centered Gaussian process f of covariance Σ^{l-1} .

Therefore, both Gaussian and orthogonal randomly initialized neural networks are in correspondence with an identical class of GPs, hereafter referred to as the Neural Networks as Gaussian Processes (NNGPs), unifying the GPs for two different initialization.

The following lemma [30] describes the Gaussian nature of the pre-activations.

Lemma 1. *Let $(W_{ij})_{n \times n}$ be an orthogonal matrix randomly sampled by the Haar measure of orthogonal matrix. Let B be a $n \times n$ matrix s.t $\text{Tr}(BB^T) = n$. Then $\text{Tr}(BW)$ converges to a standard Gaussian distribution as n tends to infinity.*

We leave the proof of pair independence of different index of pre-activations in the appendix. Here, we can observe the similarity and difference of the way Gaussian and orthogonal converge to a Gaussian process when the width of networks tends to infinity. The Gaussian process for orthogonal initialized networks can be viewed as another format of the central limit theorem as Gaussian networks, while the scale factor (variance) in the process to achieve the Gaussian process are different, which can be seen from Table 1.

4.2 Neural Tangent Kernel at initialization

According to [20], the neural tangent kernel of Gaussian weights converges in probability to a deterministic kernel in the infinite-width limit. Here we show that the NTK of network with orthogonal weights is identical to the one with Gaussian weights in the infinite width limit.

Theorem 1. *For a network of depth L at initialization, with a Lipschitz nonlinearity ϕ , and in the limit as the layers width $n_1, \dots, n_{L-1} \rightarrow \infty$, the NTK $\Theta_0^L(x, x')$, where superscript L represent the depth of a network, converges in probability to a deterministic limiting kernel:*

$$\Theta_0^L(x, x') \rightarrow \Theta_\infty^L(x, x') \otimes \mathbf{I}_{n_L \times n_L}.$$

The scalar kernel $\Theta_\infty^L(x, x') : \mathbb{R}^{n_0} \times \mathbb{R}^{n_0} \rightarrow \mathbb{R}$ is defined recursively by

$$\begin{aligned} \Theta_\infty^1(x, x') &= \Sigma^1(x, x') \\ \Theta_\infty^l(x, x') &= \sigma_w^2 \Sigma^l(x, x') \Theta_\infty^{l-1}(x, x') + \Sigma^l(x, x'), \end{aligned}$$

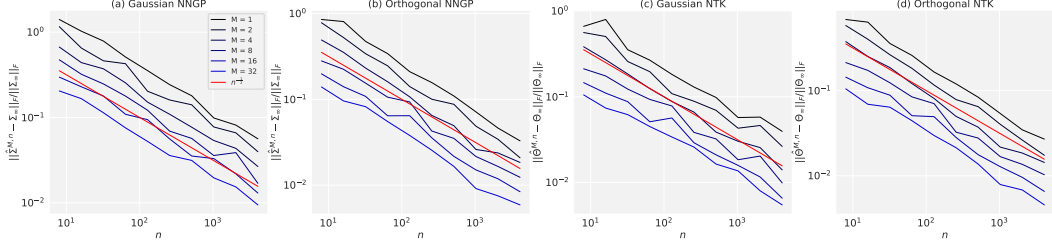


Figure 1: Kernels computed from randomly initialized ReLU networks with one hidden layer converge to the corresponding analytic kernel as width n of hidden layer and number of Monte Carlo samples M increases. The red line is an analytic function of $n^{-\frac{1}{2}}$. (a) Gaussian initialized network of NNGP. (b) the orthogonal initialized network of NNGP. (c) Gaussian initialized network of NTK. (d) Gaussian initialized network of NTK. All the kernels are consistent with convergence rate of $O(n^{-\frac{1}{2}})$.

where

$$\dot{\Sigma}^l(x, x') = \mathbb{E}_{f \sim \mathcal{N}(0, \Sigma^{(l-1)})} \left[\dot{\phi}(f(x)) \dot{\phi}(f(x')) \right],$$

taking the expectation with respect to a centered Gaussian process f of covariance Σ^{l-1} , and where $\dot{\phi}$ denotes the derivative of ϕ .

Note the neural tangent kernel of orthogonal initialized network converges to the identical deterministic kernel as Gaussian initialization. This implies that NTK of Gaussian and orthogonal neural networks are the same when the network structure (length L) and choice of hyper-parameters (ϕ , σ_w^2 , and σ_b^2) are same in the infinity width limit, and works in both ntk and standard parameterization.

We use the Monte Carlo estimates of the NNGP and NTK in the finite-width for both Gaussian and orthogonal weights to investigate the convergence rate to the infinite width kernel at initialization. We adopt the python library Neural Tangents [27] to realize calculation for Gaussian initialization and implement codes to compute those of orthogonal networks. We consider random inputs drawn from $\mathcal{N}(0, 1)$ with number training samples of $D = 20$, and dimension of input $n_0 = 1024$. The length of networks is $L = 2$ with one hidden layer. We observe convergence as the width of hidden layer $n = n_1$ increase and the number of Monte Carlo samples M increases, as shown in Figure 1. For ntk parameterization of both Gaussian and orthogonal weights, we observe,

$$\|\hat{\Sigma}^{(n)} - \Sigma_\infty\|_F = O(1/\sqrt{n}), \quad \|\hat{\Theta}^{(n)} - \Theta_\infty\|_F = O(1/\sqrt{n}), \quad (13)$$

where $\hat{\Sigma}^{(n)}$ and $\hat{\Theta}^{(n)}$ are empirical kernel with network width n . The same convergence rate for ntk parameterization for Gaussian weights have been observed by [21]. We show that the $O(1/\sqrt{n})$ convergence rate is valid for standard parameterization of both Gaussian and orthogonal weights as well in the appendix.

4.3 Neural Tangent Kernel during training

During gradient descent, NTK of Gaussian initialized networks stays asymptotically constant in the infinite-width limit as proven by [20]. This statement is equivalent to another result from [21] that networks are linearized models i.e. the first order Taylor expansion in the parameter phases. Again, we find that orthogonal initialized networks have the same conclusion, which is demonstrated below,

Theorem 2. Assume that $\lambda_{\min}(\Theta_\infty) > 0$ and $\eta_{\text{critical}} = \frac{\lambda_{\min}(\Theta_\infty) + \lambda_{\max}(\Theta_\infty)}{2}$. Let $n = n_1, \dots, n_{L-1}$ be the width of hidden layers. For a network of depth L at orthogonal initialization, with a Lipschitz nonlinearity ϕ , applying gradient descent with learning rate $\eta < \eta_{\text{critical}}$ (or gradient flow), for every input $x \in \mathbb{R}^{n_0}$ with $\|x\|_2 \leq 1$, with probability arbitrarily close to 1 over random initialization,

$$\sup_{t \geq 0} \frac{\|\theta_t - \theta_0\|_2}{\sqrt{n}}, \quad \sup_{t \geq 0} \left\| \hat{\Theta}_t - \hat{\Theta}_0 \right\|_F = O(n^{-\frac{1}{2}}), \quad \text{as } n \rightarrow \infty. \quad (14)$$

The proof of this theorem contains two main elements. One is the stability of NTK, and the other is global convergence. The original work [20] proved the stability of NTK under the assumption of

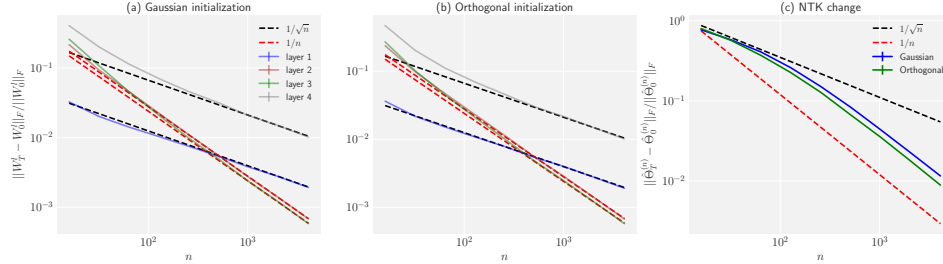


Figure 2: Changes of weights, empirical NTK on a three hidden layer Erf Network. Solid lines correspond to empirical simulation and dotted lines are theoretical predictions, i.e. black dotted lines are $1/\sqrt{n}$ while red dotted lines are $1/n$. (a) weight changes on Gaussian initialized network. (b) weight changes on the orthogonal initialized network. (c) NTK changes on both Gaussian and orthogonal networks.

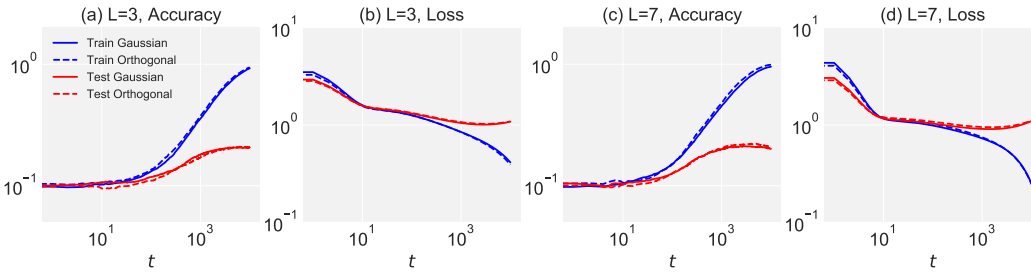


Figure 3: Dynamics of full batch gradient descent on Gaussian and orthogonal initialized networks of $T = 10^4$ steps. Orthogonal networks behaves similarly to dynamics on the corresponding Gaussian networks, for loss and accuracy functions. The dataset is selected from full CIFAR10 with $D = 256$, while MSE loss and tanh fully-connected networks are adopted for the classification task. (a)(b) Network with length $L = 3$ and width of $n = 400$, with $\sigma_w^2 = 1.5$, and $\sigma_b^2 = 0.01$. (c)(d) Network with length $L = 7$ and width of $n = 800$, with $\sigma_w^2 = 1.5$, and $\sigma_b^2 = 0.1$. While the solid lines stand for Gaussian weights, dotted lines represent orthogonal initialization.

global convergence of overparameterized neural networks, while [21] provided a self-contained proof of both global convergence and stability of NTK simultaneously. In this work, we refer to the proof strategy from [21] and extend the proof to the orthogonal case, as shown in the appendix.

We certify this theorem empirically. We use three hidden layers ReLU networks with both Gaussian and orthogonal initialization trained with learning rate $\eta = 1.0$ on a subset of MNIST dataset of $D = 20$. We measure changes of weights, empirical NTK after $T = 2^{15}$ steps of gradient descent for varying width. We observe that the relative change in first and last layer weights scales as $1/\sqrt{n}$ while second and third layer weights scale as $1/n$. This observation is valid for both Gaussian and Orthogonal weights, as shown in Figure 2(a)(b). In Figure 2(c), we find change in NTK is upper bounded by $O(1/\sqrt{n})$ but is closer to $O(1/n)$ for both Gaussian and orthogonal networks. Note that this discrepancy has been solved in [24], where they prove that relative change of empirical NTK of Gaussian initialized networks is bounded by $O(1/n)$. Without loss of generality, we infer that the proof framework is suitable for orthogonal weights.

5 Numerical experiments

In this section, we conduct a series of experiments on CIFAR10 dataset to investigate the performance of Gaussian and orthogonal initialized wide networks. Note that all the experiments in this section are performed with standard parameterization with TensorFlow. According to our theoretical result, we find that both orthogonal and Gaussian networks have the same order of convergence at initialization and during training. This means that two different initialization may have similar dynamics for loss

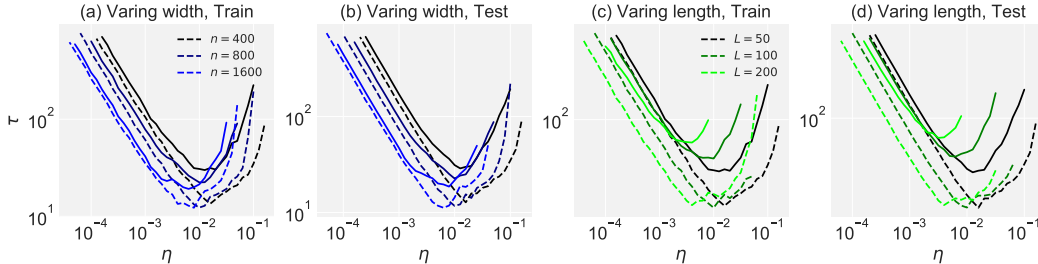


Figure 4: The steps τ as a function of learning rate η of two lines of networks on both train and test dataset. The results of the orthogonal networks are marked by dotted lines while those of Gaussian initialization are plotted by solid lines. Networks with varying width, i.e. $n = 400, 800$, and 1600 , on (a) train set and (b) test set; Networks with varying length, i.e. $L = 50, 100$, and 200 , on (c) train set and (d) test set. Different colors represent the corresponding width and length. While curves of orthogonal initialization lower than those of Gaussian initialization in the small learning rate region, the differences become more significant in the large learning rate. Besides, as networks go deeper, orthogonal initialization performs better than Gaussian’s. We average our results over 20 different instantiations of the network to reduce noise.

and accuracy function during gradient descent at low learning rate and wide width regime. We verify this intuition by providing empirical evidence with standard parameterization.

In our first numerical experiments using CIFAR10 dataset, summarized in Figure 3, we compare the dynamics, including loss and accuracy of two initialization of networks, i.e. Gaussian and orthogonal on samples of $D = 256$ dataset. We additionally average our results over 30 different instantiations of the network to reduce noise. In Figure 3(a)(b), we perform experiments on $L = 3, n = 400$, and tanh networks while conduct on $L = 7, n = 800$, and tanh networks for Figure 3(c)(d), and all the networks are optimized by gradient descent with learning rate $\eta = 0.0001$ for $T = 10^4$ steps. By comparing the loss and accuracy of Gaussian and orthogonal, we can find that the dynamics between them are nearly the same, which is consistent with the theoretical results.

However, evidence from theoretical calculation of linear network [19] and analysis on input-output Jacobian of non-linear networks [14] have shown the benefit of orthogonal initialization in the linear region of non-linear networks. This implies we need to go beyond the NTK region, where the width is large and the learning rate is small. Thus, we follow the setting of [14], where $\sigma_w^2 = 1.05$, and $\sigma_b^2 = 2.01 \times 10^{-5}$, when $\phi(x) = \tanh(x)$.

We perform two lines of experiments: (1) varying width of networks, i.e. $n = 400, 800$ and 1600 when $L = 50$; (2) varying length of networks, i.e. $L = 50, 100$ and 200 , when $n = 400$, using SGD optimizer on complete CIFAR10. To investigate the relationship between learning rate and train speed, we select a threshold accuracy of $p = 0.25$ and measure the first step τ when performance exceeds p . We show the steps τ as a function of learning rate η of two lines of networks on both train and test dataset in Figure 4.

There are two main conclusions we can obtain from the results of experiments. First, the orthogonal initialization can outperform Gaussian ones in the large learning rate region on both train and test dataset. Notably, the out-performance happens at the trough of the learning curve, which is the optimal learning rate. Second, the difference in performance between orthogonal and Gaussian initialization with a settings of linear regime of nonlinear activations is more significant when the networks go deeper.

6 Conclusion

In this work, we study the neural tangent kernel of wide and non-linear networks with orthogonal initialization. We prove that the NTK of orthogonal initialized networks converges to the same deterministic kernel in the infinite width limit at initialization as Gaussian initialized networks. During training via gradient descent (gradient flow), we find that the NTK of orthogonal initialization stays unchanged in the infinite width limit and have the same order convergence rate from finite

width to the infinite limit as Gaussian networks. The theoretical results imply that the dynamics of wide networks with orthogonal initialization behave similarly as those of Gaussian networks at a small learning rate, which is verified by experiments. Finally, we find that orthogonal networks can outperform the Gaussian's in the large learning rate and depth on both train and test set in a linear regime of nonlinear activations. We leave the theoretical investigation on the large learning rate region and generalization ability in the future.

References

- [1] Mark Nixon and Alberto Aguado. *Feature extraction and image processing for computer vision*. Academic Press, 2019.
- [2] Jacob Devlin, Ming-Wei Chang, Kenton Lee, and Kristina Toutanova. Bert: Pre-training of deep bidirectional transformers for language understanding. *arXiv preprint arXiv:1810.04805*, 2018.
- [3] Volodymyr Mnih, Koray Kavukcuoglu, David Silver, Andrei A Rusu, Joel Veness, Marc G Bellemare, Alex Graves, Martin Riedmiller, Andreas K Fidjeland, Georg Ostrovski, et al. Human-level control through deep reinforcement learning. *Nature*, 518(7540):529–533, 2015.
- [4] Kaiming He, Xiangyu Zhang, Shaoqing Ren, and Jian Sun. Deep residual learning for image recognition. In *Proceedings of the IEEE conference on computer vision and pattern recognition*, pages 770–778, 2016.
- [5] Nitish Srivastava, Geoffrey Hinton, Alex Krizhevsky, Ilya Sutskever, and Ruslan Salakhutdinov. Dropout: a simple way to prevent neural networks from overfitting. *The journal of machine learning research*, 15(1):1929–1958, 2014.
- [6] Sergey Ioffe and Christian Szegedy. Batch normalization: Accelerating deep network training by reducing internal covariate shift. *arXiv preprint arXiv:1502.03167*, 2015.
- [7] Ben Poole, Subhaneil Lahiri, Maithra Raghu, Jascha Sohl-Dickstein, and Surya Ganguli. Exponential expressivity in deep neural networks through transient chaos. In *Advances in neural information processing systems*, pages 3360–3368, 2016.
- [8] Samuel S Schoenholz, Justin Gilmer, Surya Ganguli, and Jascha Sohl-Dickstein. Deep information propagation. *arXiv preprint arXiv:1611.01232*, 2016.
- [9] Lechao Xiao, Yasaman Bahri, Jascha Sohl-Dickstein, Samuel S Schoenholz, and Jeffrey Pennington. Dynamical isometry and a mean field theory of cnns: How to train 10,000-layer vanilla convolutional neural networks. *arXiv preprint arXiv:1806.05393*, 2018.
- [10] Minmin Chen, Jeffrey Pennington, and Samuel S Schoenholz. Dynamical isometry and a mean field theory of rnns: Gating enables signal propagation in recurrent neural networks. *arXiv preprint arXiv:1806.05394*, 2018.
- [11] Wei Huang, Richard Yi Da Xu, Weitao Du, Yutian Zeng, and Yunce Zhao. Mean field theory for deep dropout networks: digging up gradient backpropagation deeply. *arXiv preprint arXiv:1912.09132*, 2019.
- [12] Ge Yang and Samuel Schoenholz. Mean field residual networks: On the edge of chaos. In *Advances in neural information processing systems*, pages 7103–7114, 2017.
- [13] Greg Yang, Jeffrey Pennington, Vinay Rao, Jascha Sohl-Dickstein, and Samuel S Schoenholz. A mean field theory of batch normalization. *arXiv preprint arXiv:1902.08129*, 2019.
- [14] Jeffrey Pennington, Samuel Schoenholz, and Surya Ganguli. Resurrecting the sigmoid in deep learning through dynamical isometry: theory and practice. In *Advances in neural information processing systems*, pages 4785–4795, 2017.
- [15] Jeffrey Pennington, Samuel S Schoenholz, and Surya Ganguli. The emergence of spectral universality in deep networks. *arXiv preprint arXiv:1802.09979*, 2018.

- [16] Andrew M Saxe, James L McClelland, and Surya Ganguli. Exact solutions to the nonlinear dynamics of learning in deep linear neural networks. *arXiv preprint arXiv:1312.6120*, 2013.
- [17] Wojciech Tarnowski, Piotr Warchoł, Stanisław Jastrzębski, Jacek Tabor, and Maciej A Nowak. Dynamical isometry is achieved in residual networks in a universal way for any activation function. *arXiv preprint arXiv:1809.08848*, 2018.
- [18] Zenan Ling and Robert C Qiu. Spectrum concentration in deep residual learning: a free probability approach. *IEEE Access*, 7:105212–105223, 2019.
- [19] Wei Hu, Lechao Xiao, and Jeffrey Pennington. Provable benefit of orthogonal initialization in optimizing deep linear networks. *arXiv preprint arXiv:2001.05992*, 2020.
- [20] Arthur Jacot, Franck Gabriel, and Clément Hongler. Neural tangent kernel: Convergence and generalization in neural networks. In *Advances in neural information processing systems*, pages 8571–8580, 2018.
- [21] Jaehoon Lee, Lechao Xiao, Samuel Schoenholz, Yasaman Bahri, Roman Novak, Jascha Sohl-Dickstein, and Jeffrey Pennington. Wide neural networks of any depth evolve as linear models under gradient descent. In *Advances in neural information processing systems*, pages 8570–8581, 2019.
- [22] Piotr A Sokol and Il Memming Park. Information geometry of orthogonal initializations and training. *arXiv preprint arXiv:1810.03785*, 2018.
- [23] Greg Yang. Scaling limits of wide neural networks with weight sharing: Gaussian process behavior, gradient independence, and neural tangent kernel derivation. *arXiv preprint arXiv:1902.04760*, 2019.
- [24] Jiaoyang Huang and Horng-Tzer Yau. Dynamics of deep neural networks and neural tangent hierarchy. *arXiv preprint arXiv:1909.08156*, 2019.
- [25] Sanjeev Arora, Simon S Du, Wei Hu, Zhiyuan Li, Russ R Salakhutdinov, and Ruosong Wang. On exact computation with an infinitely wide neural net. In *Advances in Neural Information Processing Systems*, pages 8139–8148, 2019.
- [26] Jascha Sohl-Dickstein, Roman Novak, Samuel S Schoenholz, and Jaehoon Lee. On the infinite width limit of neural networks with a standard parameterization. *arXiv preprint arXiv:2001.07301*, 2020.
- [27] Roman Novak, Lechao Xiao, Jiri Hron, Jaehoon Lee, Alexander A. Alemi, Jascha Sohl-Dickstein, and Samuel S. Schoenholz. Neural tangents: Fast and easy infinite neural networks in python. <https://github.com/google/neural-tangents>, <https://arxiv.org/abs/1912.02803>, 2019.
- [28] Jaehoon Lee, Yasaman Bahri, Roman Novak, Samuel S Schoenholz, Jeffrey Pennington, and Jascha Sohl-Dickstein. Deep neural networks as gaussian processes. *arXiv preprint arXiv:1711.00165*, 2017.
- [29] Alexander G de G Matthews, Mark Rowland, Jiri Hron, Richard E Turner, and Zoubin Ghahramani. Gaussian process behaviour in wide deep neural networks. *arXiv preprint arXiv:1804.11271*, 2018.
- [30] Sourav Chatterjee and Elizabeth Meckes. Multivariate normal approximation using exchangeable pairs. *arXiv preprint math/0701464*, 2007.

A Appendix

This appendix is dedicated to proving the key results of this paper, namely Proposition 1 and Theorems 1 and 2, which describe the asymptotics of neural networks with orthogonal weights at initialization and during training. Besides, we provide more experiments regarding to standard parameterization.

A.1 NNGP at Initialization

We follow the proof strategy of [20] to take the limit as $n_1, \dots, n_{L-1} \rightarrow \infty$ sequentially. Before proof, we list two critical lemma from [30]:

Lemma 1. *Let $(W_{ij})_{n \times n}$ be an orthogonal matrix randomly sampled by the Haar measure of orthogonal matrix. Let B be a $n \times n$ matrix s.t $\text{Tr}(BB^T) = n$. Then $\text{Tr}(BW)$ converges to a standard Gaussian distribution as n tends to infinity.*

Lemma 2. *If $(W_{ij})_{n \times n}$ is an orthogonal matrix distributed according to Haar measure, then $\mathbb{E} \left[\prod W_{ij}^{k_{ij}} \right]$ is non-zero if and only if the number of entries from each row and from each column is even. Second and fourth-degree moments are as follows:*

1. For all i, j ,

$$\mathbb{E} [W_{ij}^2] = \frac{1}{n}.$$

2. For all $i, j, r, s, \alpha, \beta, \lambda, \mu$,

$$\begin{aligned} \mathbb{E} [W_{ij} W_{rs} W_{\alpha\beta} W_{\lambda\mu}] &= -\frac{1}{(n-1)n(n+2)} \left[\delta_{ir} \delta_{\alpha\lambda} \delta_{j\beta} \delta_{s\mu} + \delta_{ir} \delta_{\alpha\lambda} \delta_{j\mu} \delta_{s\beta} + \delta_{i\alpha} \delta_{r\lambda} \delta_{js} \delta_{\beta\mu} \right. \\ &\quad \left. + \delta_{i\alpha} \delta_{r\lambda} \delta_{j\mu} \delta_{\beta s} + \delta_{i\lambda} \delta_{r\alpha} \delta_{js} \delta_{\beta\mu} + \delta_{i\lambda} \delta_{r\alpha} \delta_{j\beta} \delta_{s\mu} \right] \\ &\quad + \frac{n+1}{(n-1)n(n+2)} \left[\delta_{ir} \delta_{\alpha\lambda} \delta_{js} \delta_{\beta\mu} + \delta_{i\alpha} \delta_{r\lambda} \delta_{j\beta} \delta_{s\mu} + \delta_{i\lambda} \delta_{r\alpha} \delta_{j\mu} \delta_{s\beta} \right]. \end{aligned}$$

Proposition 1. *For a network of depth L at initialization, with a Lipschitz nonlinearity ϕ , and in the limit as $n_1, \dots, n_{L-1} \rightarrow \infty$, the pre-activation h_i^l , for $i = 1, \dots, n_l$, tend to i.i.d centered Gaussian processes of covariance Σ^l , where Σ^l is defined recursively by:*

$$\begin{aligned} \Sigma^1(x, x') &= \frac{\sigma_w^2}{n_0} x^T x' + \sigma_b^2 \\ \Sigma^l(x, x') &= \sigma_w^2 \mathbb{E}_{f \sim \mathcal{N}(0, \Sigma^{l-1})} [\phi(f(x)) \phi(f(x'))] + \sigma_b^2, \end{aligned}$$

taking the expectation with respect to a centered Gaussian process f of covariance Σ^{l-1} .

Proof. We prove the result by induction for the ntk parameterization, while the proof for standard parameterization can be derived in the same way. When $L = 1$, there are no hidden layers and h_i^1 has the form:

$$h_i^1 = \sum_{j=1}^{n_0} \frac{\sigma_w}{\sqrt{n_0}} W_{ij}^1 x_j^0 + \sigma_b \beta_i^1.$$

Then we check the variance Σ^1 of output layer h_i^1 . By Lemma 2,

$$\mathbb{E} [W_{ij}^1] = 0, \quad \mathbb{E} [W_{ij}^1 W_{kl}^1] = \frac{1}{n_0} n_0 \delta_{ik} \delta_{jl} = \delta_{ik} \delta_{jl}.$$

We note that the fraction $\frac{1}{n_0}$ is from the integration on orthogonal distribution while the term n_0 comes from initialization. Thus we can compute the covariance of the first layer,

$$\begin{aligned} \Sigma^1 &= \mathbb{E} [h_i^1 h_i^1] = \mathbb{E} \left[\left(\sum_{j=1}^{n_0} \frac{\sigma_w}{\sqrt{n_0}} W_{ij}^1 x_j^0 + \sigma_b \beta_i^1 \right) \left(\sum_{j'=1}^{n_0} \frac{\sigma_w}{\sqrt{n_0}} W_{ij'}^1 x_{j'}^0 + \sigma_b \beta_i^1 \right) \right] \\ &= \frac{\sigma_w^2}{n_0} \mathbb{E} \left[\sum_{j=1}^{n_0} \sum_{j'=1}^{n_0} W_{ij}^1 x_j^0 W_{ij'}^1 x_{j'}^0 \right] + \sigma_b^2 = \frac{\sigma_w^2}{n_0} x^T x + \sigma_b^2. \end{aligned}$$

The next step is to use induction method. Consider an l -network as the function mapping the input to the pre-activations h_i^l . The induction hypothesis gives that in the limit as sequentially

$n_1, \dots, n_{l-2} \rightarrow \infty$ the preactivations h_i^{l-1} tend to i.i.d Gaussian processes with covariance Σ^{l-1} . The outputs is govern by,

$$h_i^l = \frac{\sigma_w}{\sqrt{n_{l-1}}} \sum_{j=1}^{n_{l-1}} W_{ij}^l x_j^{l-1} + \sigma_b \beta_i^l$$

By the Lemma 1, let $B = \sqrt{\frac{n_{l-1}}{\sum_{i=1}^{n_{l-1}} (x_i^{l-1})^2}} \begin{bmatrix} x_1^{l-1} & 0 & \cdots & 0 \\ \vdots & \vdots & \ddots & \vdots \\ x_{n_{l-1}}^{l-1} & 0 & \cdots & 0 \end{bmatrix}$, thus $\text{tr}(BB^T) = n_{l-1}$. Then we

have $\lim_{n \rightarrow \infty} \sum_{j=1}^{n_{l-1}} \frac{1}{\sqrt{n_{l-1}}} W_{ij}^l x_j^{l-1}$ tends to $\mathcal{N}(0, \lim_{n \rightarrow \infty} \frac{\sum_{i=1}^{n_{l-1}} (x_i^{l-1})^2}{n_{l-1}})$.

As a result, h_i^l are centered Gaussian with covariance,

$$\Sigma^l(x, x') = \frac{\sigma_w^2}{n_{l-1}} \sum_j \phi(h_j^{l-1}(x)) \phi(h_j^{l-1}(x')) + \sigma_b^2$$

Since h_j^{l-1}, h_k^{l-1} are independent for $j \neq k$, we have

$$\text{Var}(\Sigma^l(x, x')) = \frac{\sigma_w^4}{n_{l-1}^2} \sum_j \mathbb{E}[\phi(h_j^{l-1}(x))^2 \phi(h_j^{l-1}(x'))^2] - \frac{\sigma_w^4}{n_{l-1}^2} \sum_j \mathbb{E}[\phi(h_j^{l-1}(x)) \phi(h_j^{l-1}(x'))]^2$$

by the symmetry on the underlying index j , we can choose index 1 as a representative,

$$\text{Var}(\Sigma^l(x, x')) = \frac{\sigma_w^4}{n_{l-1}} \mathbb{E}[\phi(h_1^{l-1}(x))^2 \phi(h_1^{l-1}(x'))^2] - \frac{\sigma_w^4}{n_{l-1}} \mathbb{E}[\phi(h_1^{l-1}(x)) \phi(h_1^{l-1}(x'))]^2$$

Since $\mathbb{E}[\phi(h_1^{l-1}(x))^2 \phi(h_1^{l-1}(x'))^2] - \mathbb{E}[\phi(h_1^{l-1}(x)) \phi(h_1^{l-1}(x'))]$ is bounded, by the Chebyshev's inequality, the covariance kernel tends in probability to the expectation,

$$\Sigma^l(x, x') = \sigma_w^2 \mathbb{E}_{f \sim \mathcal{N}(0, \Sigma^{l-1})}[\phi(f(x)) \phi(f(x'))] + \sigma_b^2.$$

We still need to verify the independence of h_i^l, h_j^l for $i \neq j$. This follows from computing the covariance between h_i^l, h_j^l :

$$\lim_{n_{l-1} \rightarrow \infty} \text{Cov}(h_i^l(x) h_j^l(x')) = \sum_k \sum_l W_{ik}^l \phi(h_k^{l-1}(x)) W_{jl}^l \phi(h_l^{l-1}(x'))$$

Note that we ignore the bias b_i^l , since they are independent with the W_{ij}^l . By the Lemma 2,

$$\mathbb{E}[W_{ik} W_{jl}] = 0, \text{ for } i \neq j$$

thus we have,

$$\lim_{n_{l-1} \rightarrow \infty} \text{Cov}(h_i^l(x) h_j^l(x')) = 0$$

Since we know as $n_{l-1} \rightarrow \infty$, $h_i^l(x), h_j^l(x')$ are Gaussian, zero covariance means they are independent. □

A.2 NTK at Initialization

In the infinite-width limit, the neural tangent kernel which is random at networks with orthogonal initialization, converges in probability to a deterministic limit.

Theorem 1. *For a network of depth L at initialization, with a Lipschitz nonlinearity ϕ , and in the limit as the layers width $n_1, \dots, n_{L-1} \rightarrow \infty$, the NTK $\Theta_0^L(x, x')$, where superscript L represent the depth of a network, converges in probability to a deterministic limiting kernel:*

$$\Theta_0^L(x, x') \rightarrow \Theta_\infty^L(x, x') \otimes \mathbf{I}_{n_L \times n_L}.$$

The scalar kernel $\Theta_\infty^L(x, x') : \mathbb{R}^{n_0} \times \mathbb{R}^{n_0} \rightarrow \mathbb{R}$ is defined recursively by

$$\begin{aligned}\Theta_\infty^1(x, x') &= \Sigma^1(x, x') \\ \Theta_\infty^l(x, x') &= \sigma_w^2 \dot{\Sigma}^l(x, x') \Theta_\infty^{l-1}(x, x') + \Sigma^l(x, x'),\end{aligned}$$

where

$$\dot{\Sigma}^l(x, x') = \mathbb{E}_{f \sim \mathcal{N}(0, \Sigma^{l-1})} \left[\dot{\phi}(f(x)) \dot{\phi}(f(x')) \right],$$

taking the expectation with respect to a centered Gaussian process f of covariance Σ^{l-1} , and where $\dot{\phi}$ denotes the derivative of ϕ .

Proof. We prove the result by induction for the ntk parameterization, while the proof for standard parameterization can be derived in the same way with a similar result, see the details for the Gaussian initialization [26]. For the input layer $L = 1$, take the derivative with respect to W_{ij}^1, b_j^1 , we have

$$\begin{aligned}\Theta_{kk'}^1(x, x') &= \frac{\sigma_w^2}{n_0} \sum_{i=1}^{n_0} \sum_{j=1}^{n_0} x_i x'_i \delta_{jk} \delta_{jk'} + \sigma_b^2 \sum_{j=1}^{n_0} \delta_{jk} \delta_{jk'} \\ &= \frac{\sigma_w^2}{n_0} x^T x' \delta_{kk'} + \sigma_b^2 \delta_{kk'}\end{aligned}$$

From $l-1$ to l , by the induction hypothesis, as $n_1, \dots, n_{l-2} \rightarrow \infty$, the pre-activations h_i^{l-1} are i.i.d centered Gaussian with covariance Σ^{l-1} and $\Theta_{ii'}^{l-1}(x, x')$ converges to:

$$(\partial_\theta h_i^{l-1}(x))^T (\partial_\theta h_{i'}^{l-1}(x')) \rightarrow \Theta_\infty^{l-1}(x, x') \delta_{ii'}.$$

Now we calculate the NTK for l -layer networks, and divide the parameters into two parts. One only involves the parameters of the l layer, and the other is the collect of parameters of previous $l-1$ layers. The first part of the NTK is given by,

$$\partial_{w^l} h_k^l(x) \cdot \partial_{w^l} h_k^l(x') + \partial_{b^l} h_k^l(x) \cdot \partial_{b^l} h_k^l(x') = \frac{\sigma_w^2}{n_{l-1}} \phi(h^l(x)) \phi(h^l(x')) + \sigma_b^2$$

We have proved in the proposition 1 that $n_{l-1} \rightarrow \infty$, it tends to $\Sigma^l(x, x')$.

For the second part, denoting the parameters of the previous $l-1$ layers as $\tilde{\theta}$, we have

$$\partial_{\tilde{\theta}} h_k^l(x) = \frac{\sigma_w}{\sqrt{n_{l-1}}} \sum_{i=1}^{n_{l-1}} \partial_{\tilde{\theta}} h_i^{l-1}(x) \dot{\phi}(h_i^{l-1}(x)) W_{ik}^l$$

By the induction hypothesis that the NTK of $(l-1)$ -layer networks $\Theta_{kk'}^{l-1}(x, x')$ converges to a diagonal kernel as $n_1, \dots, n_{l-2} \rightarrow \infty$, we have the second part of NTK as,

$$\frac{\sigma_w^2}{n_{l-1}} \sum_{i, i'=1}^{n_{l-1}} \Theta_{ii'}^{l-1}(x, x') \dot{\phi}(h_i^{l-1}(x)) \dot{\phi}(h_{i'}^{l-1}(x')) W_{ik}^l W_{i'k'}^l \rightarrow \frac{\sigma_w^2}{n_{l-1}} \sum_{i=1}^{n_{l-1}} \Theta_\infty^{l-1}(x, x') \dot{\phi}(h_i^{l-1}(x)) \dot{\phi}(h_i^{l-1}(x')) W_{ik}^l W_{ik'}^l$$

Denote the right hand side as α , by the Lemma 2,

$$\mathbb{E}[\alpha] = \frac{\sigma_w^2}{n_{l-1}} \delta_{kk'} \sum_{i=1}^{n_{l-1}} \Theta_{ii'}^{l-1}(x, x') \dot{\phi}(h_i^{l-1}(x)) \dot{\phi}(h_{i'}^{l-1}(x'))$$

$$\text{Var}(\alpha) = \mathbb{E}[(\alpha - \mathbb{E}[\alpha])^2] = \frac{\sigma_w^4}{n_{l-1}^2} \mathbb{E} \left[\left(\sum_{i=1}^{n_{l-1}} \Theta_\infty^{l-1}(x, x') \dot{\phi}(h_i^{l-1}(x)) \dot{\phi}(h_i^{l-1}(x')) (W_{ik}^l W_{ik'}^l - \delta_{kk'}) \right)^2 \right]$$

Expanding the square, the sum is decomposed into the two parts according to the index. For the terms with the same first index i , we have

$$\mathbb{E}[(W_{ik}^l W_{ik'}^l - \delta_{kk'})^2] = \mathbb{E}[W_{ik}^l W_{ik'}^l]^2 - \delta_{kk'}$$

Note that the weights are drawn from the ntk parameterization, and by the Lemma 2,

$$\mathbb{E}[(W_{ik}^l)^2 (W_{ik'}^l)^2] \sim O(1)$$

so the terms with the same index i are of order $O(\frac{1}{n_{l-1}})$:

$$\frac{\sigma_w^4}{n_{l-1}^2} \mathbb{E} \left[\sum_{i=1}^{n_{l-1}} (\Theta_{\infty}^{l-1}(x, x') \dot{\phi}(h_i^{l-1}(x)) \dot{\phi}(h_i^{l-1}(x')))^2 (W_{ik}^l W_{ik'}^l - \delta_{kk'})^2 \right] \sim O\left(\frac{1}{n_{l-1}}\right)$$

For the terms with differential index i , we need to estimate

$$\gamma := \mathbb{E}[(W_{ik}^l W_{ik'}^l - \delta_{kk'})(W_{i'k}^l W_{i'k'}^l - \delta_{kk'})]$$

If $k = k'$, by the Lemma 2 on the fourth moment,

$$\gamma = -\frac{2n_{l-1}^2}{(n_{l-1} - 1)n_{l-1}(n_{l-1} + 2)} + \frac{(n_{l-1} + 1)n_{l-1}^2}{(n_{l-1} - 1)n_{l-1}(n_{l-1} + 2)} - 1 \sim O\left(\frac{1}{n_{l-1}}\right)$$

If $k \neq k'$,

$$\mathbb{E}[(W_{ik} W_{ik'} W_{i'k} W_{i'k'})] = -\frac{n_{l-1}^2}{(n_{l-1} - 1)n_{l-1}(n_{l-1} + 2)} \sim O\left(\frac{1}{n_{l-1}}\right)$$

In each case, both $\gamma \sim O(\frac{1}{n_{l-1}})$, thus we have,

$$\frac{\sigma_w^4}{n_{l-1}^2} \mathbb{E} \left[\sum_{i=1}^{n_{l-1}} \sum_{i'=1}^{n_{l-1}} (\Theta_{\infty}^{l-1}(x, x') \dot{\phi}(h_i^{l-1}(x)) \dot{\phi}(h_{i'}^{l-1}(x')))^2 (W_{ik}^l W_{i'k'}^l - \delta_{kk'})^2 \right] \sim O\left(\frac{1}{n_{l-1}}\right)$$

Combining the two parts, we have

$$\text{Var}(\alpha) \sim O\left(\frac{1}{n_{l-1}}\right)$$

By Chebyshev's inequality, α tends to its mean as $n_{l-1} \rightarrow \infty$, which is

$$\lim_{n_{l-1} \rightarrow \infty} \frac{\sigma_w^2}{n_{l-1}} \delta_{kk'} \sum_i \Theta_{\infty}^{l-1}(x, x') \dot{\phi}(h_i^{l-1}(x)) \dot{\phi}(h_i^{l-1}(x')) = \sigma_w^2 \Theta_{\infty}^{l-1}(x, x') \dot{\Sigma}^l(x, x') \delta_{kk'}$$

Combining this with the first part of NTK, we have

$$\Theta_{\infty}^l(x, x') = \sigma_w^2 \Theta_{\infty}^{l-1}(x, x') \dot{\Sigma}^l(x, x') + \Sigma^l(x, x')$$

□

A.3 NTK during training

The NTK of networks with orthogonal initialization stays constant during training in the infinite-width limit. More precisely, we can give an upper bound for the change of parameters and NTK at wide width.

Theorem 2. Assume that $\lambda_{\min}(\Theta_{\infty}) > 0$ and $\eta_{\text{critical}} = \frac{\lambda_{\min}(\Theta_{\infty}) + \lambda_{\max}(\Theta_{\infty})}{2}$. Let $n = n_1, \dots, n_{L-1}$ be the width of hidden layers. For a network of depth L at orthogonal initialization, with a Lipschitz nonlinearity ϕ , applying gradient descent with learning rate $\eta < \eta_{\text{critical}}$ (or gradient flow), for every input $x \in \mathbb{R}^{n_0}$ with $\|x\|_2 \leq 1$, with probability arbitrarily close to 1 over random initialization,

$$\sup_{t \geq 0} \frac{\|\theta_t - \theta_0\|_2}{\sqrt{n}}, \sup_{t \geq 0} \left\| \hat{\Theta}_t - \hat{\Theta}_0 \right\|_F = O(n^{-\frac{1}{2}}), \text{ as } n \rightarrow \infty. \quad (15)$$

We first prove the *local Lipschitzness* of $J(\theta) := \nabla_{\theta} h^L(\theta) \in \mathbb{R}^{(D_{n_L}) \times |\theta|}$, where $|\theta|$ is the number of parameters. Once we have the upper bound of $J(\theta)$, the stability comes from proving that the difference is small of the NTK from time t to time $t + 1$. As it has been observed in [21], this step is universal of the network structure and also the initialization. Thus, our primary target is construct local Lipschitzness of orthogonal initialization. The Lemma below illustrates the local Lipschitzness of $J(\theta)$ without scale condition for the input layer.

Lemma 3. (local Lipschitzness of $J(\theta)$) $\exists K > 0$ s.t for every $c > 0$, $\exists n_c$ s.t for $n \geq n_c$, we have the following bound:

$$\begin{cases} \|J(\theta) - J(\tilde{\theta})\|_F \leq K \|\theta - \tilde{\theta}\|_2, \\ \|J(\theta)\|_F \leq K, \end{cases}, \forall \theta, \tilde{\theta} \in B(\theta_0, \frac{c}{n}) \quad (16)$$

Where

$$B(\theta_0, R) := \{\theta : \|\theta - \theta_0\|_2 < R\}.$$

Proof. We prove the result by induction for the standard parameterization, while the proof for ntk parameterization can be derived in the same way. For $l \geq 1$, let

$$\delta^l(\theta, x) := \nabla_{h^l(\theta, x)} h^L(x) \in \mathbb{R}^{n_L n}$$

$$\delta^l(\theta, X) := \nabla_{h^l(\theta, X)} h^L(X) \in \mathbb{R}^{(n_L D) \times (n_L D)}$$

Let $\theta = \{W^l, b^l\}$, $\tilde{\theta} = \{\tilde{W}^l, \tilde{b}^l\}$ be two points in $B(\theta_0, \frac{c}{n})$. Since the initialization is to choose an orthogonal matrix, i.e. $W^T W = \sigma_w^2 \mathbf{I}$. If the width n is large enough, we have,

$$\|W^l\|_{op}, \|\tilde{W}^l\|_{op} \leq 3\sigma_w \quad \text{for all } l.$$

As in the original proof for Gaussian initialization [21], there is a constant K_1 , depending on D , σ_w^2 , σ_b^2 , and number of layers L s.t with high probability over orthogonal initialization,

$$\|x^l(\theta, X)\|_2, \|\delta^l(\theta, X)\|_2 \leq K_1$$

$$\|x^l(\theta, X) - x^l(\tilde{\theta}, X)\|_2, \|\delta^l(\theta, X) - \delta^l(\tilde{\theta}, X)\|_2 \leq K_1 \|\tilde{\theta} - \theta\|_2$$

Note: there is a scaling factor $\frac{1}{\sqrt{n}}$ along with $\|x^l(\theta, X)\|_2$ in the Gaussian case, since from the input layer to the first layer, for the Gaussian initialization, we have

$$\|W^1\|_{op}, \|\tilde{W}^1\|_{op} \leq 3\sigma_w \frac{\sqrt{n}}{\sqrt{n_0}}.$$

Decomposing the $J(\theta)$ into two parts, we have

$$\begin{aligned} \|J(\theta)\|_F^2 &= \sum_l \|\nabla_{W^l} h^L(\theta)\|_F^2 + \|\nabla_{b^l} h^L(\theta)\|_F^2 \\ &= \sum_l \sum_{x \in X} \|x^{l-1}(\theta, x) \delta^l(\theta, x)^T\|_F^2 + \|\delta^l(\theta, x)^T\|_F^2 \\ &\leq \sum_l \sum_{x \in X} (1 + \|x^{l-1}(\theta, x) \delta^l(\theta, x)^T\|_F^2) \cdot \|\delta^l(\theta, x)^T\|_F^2 \\ &\leq \sum_l (1 + K_1^2) \sum_x \|\delta^l(\theta, x)^T\|_F^2 \\ &\leq 2LK_1^4 \end{aligned}$$

and similarly,

$$\begin{aligned} \|J(\theta) - J(\tilde{\theta})\|_F^2 &= \sum_l \sum_{x \in X} \|x^{l-1}(\theta, x) \delta^l(\theta, x)^T - x^{l-1}(\tilde{\theta}, x) \delta^l(\tilde{\theta}, x)^T\|_F^2 + \|\delta^l(\theta, x)^T - \delta^l(\tilde{\theta}, x)^T\|_F^2 \\ &= \sum_l \sum_{x \in X} \|x^{l-1}(\theta, x) \delta^l(\theta, x)^T - x^{l-1}(\tilde{\theta}, x) \delta^l(\theta, x)^T\|_F^2 \\ &\quad + \|x^{l-1}(\tilde{\theta}, x) \delta^l(\theta, x)^T - x^{l-1}(\tilde{\theta}, x) \delta^l(\tilde{\theta}, x)^T\|_F^2 + \|\delta^l(\theta, x)^T - \delta^l(\tilde{\theta}, x)^T\|_F^2 \\ &\leq \sum_l 2K_1^4 \|\tilde{\theta} - \theta\|^2 + K_1^2 \|\tilde{\theta} - \theta\|^2 \\ &\leq 3K_1^4 L \|\tilde{\theta} - \theta\|^2 \end{aligned}$$

□

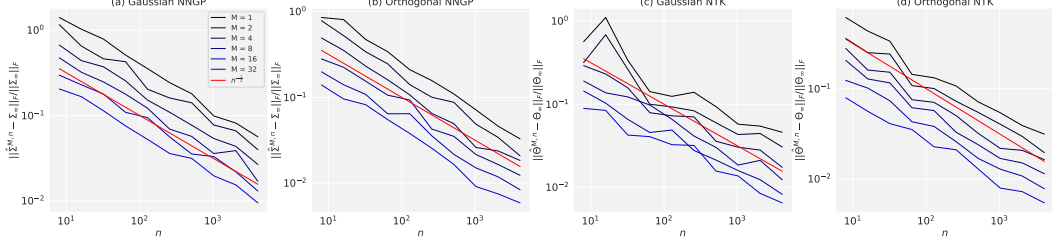


Figure 5: Kernels with standard parameterization computed from randomly initialized ReLU networks with one hidden layers converge to the corresponding analytic kernel as width n of hidden layer and number of Monte Carlo samples M increases. The red line is an analytic function of $n^{-\frac{1}{2}}$. (a) Gaussian initialized network of NNGP. (b) orthogonal initialized network of NTK. (c) Gaussian initialized network of NTK. (d) Gaussian initialized network of NTK. All the kernels are consistent with convergence rate of $O(n^{-\frac{1}{2}})$.

Note: In our setting, since we want the orthogonal and Gaussian initialization have the same NTK, we need to scale the initialization for the input layer:

$$(W^1)^T W^1 = \sigma_w^2 \frac{n}{n_0}, \quad W^1 \in \mathbb{R}^{n \times n_0}$$

If we impose this condition, then,

$$\|W^1\|_{op}, \quad \|\tilde{W}^1\|_{op} \leq 3\sigma_w \frac{\sqrt{n}}{\sqrt{n_0}}$$

So we recover the same lipschitz constant as in the Gaussian initialization condition:

Corollary 1. (local Lipschitzness of $J(\theta)$ with scale condition) Under the above scaling condition on the input layer, $\exists K > 0$ s.t for every $c > 0$, $\exists n_c$ s.t for $n \geq n_c$, we have the following bound: $\exists K > 0$ s.t for every $c > 0$, $\exists n_c$ s.t for $n \geq n_c$, we have the following bound:

$$\begin{cases} \frac{1}{\sqrt{n}} \|J(\theta) - J(\tilde{\theta})\|_F \leq K \|\theta - \tilde{\theta}\|_2, \\ \frac{1}{\sqrt{n}} \|J(\theta)\|_F \leq K, \end{cases}, \forall \theta, \tilde{\theta} \in B(\theta_0, \frac{c}{\sqrt{n}}) \quad (17)$$

Where $B(\theta_0, R) := \{\theta : \|\theta - \theta_0\|_2 < R\}$.

With this Corollary, the left proof for Theorem 2 is exact same as that of Theorem G.1 and Theorem G.2 for Gaussian initialization in [21].

A.4 Convergence of empirical kernel with standard parameterization

We use the Monte Carlo estimates of the NNGP and NTK in the finite-width for both Gaussian and orthogonal weights at initialization with standard parameterization. We adopt the python library Neural Tangents [27] to realize calculation for Gaussian initialization and implement codes to compute those of orthogonal networks. We consider random inputs drawn from $\mathcal{N}(0, 1)$ with number training samples of $D = 20$, and dimension of input $n_0 = 1024$. The length of networks is $L = 2$ with one hidden layer. We observe convergence as width of hidden layer $n = n_1$ increase and the number of Monte Carlo samples M increases, as shown in Figure 5. Again, for standard parameterization of both Gaussian and orthogonal weights, we observe,

$$\|\hat{\Sigma}^{(n)} - \Sigma_\infty\|_F = O(1/\sqrt{n}), \quad \|\hat{\Theta}^{(n)} - \Theta_\infty\|_F = O(1/\sqrt{n}). \quad (18)$$